Hiking down the Energy Landscape: Progress Toward the Kauzmann Temperature via Vapor Deposition

Kenneth L. Kearns, Stephen F. Swallen, and M. D. Ediger*

Department of Chemistry, University of Wisconsin—Madison, Madison, Wisconsin, 53706

Tian Wu,† Ye Sun, and Lian Yu

School of Pharmacy, University of Wisconsin—Madison, Madison, Wisconsin, 53705

Received: November 30, 2007; In Final Form: January 17, 2008

Physical vapor deposition was employed to prepare amorphous samples of indomethacin and 1,3,5-(tris)-naphthylbenzene. By depositing onto substrates held somewhat below the glass transition temperature and varying the deposition rate from 15 to 0.2 nm/s, glasses with low enthalpies and exceptional kinetic stability were prepared. Glasses with fictive temperatures that are as much as 40 K lower than those prepared by cooling the liquid can be made by vapor deposition. As compared to an ordinary glass, the most stable vapor-deposited samples moved about 40% toward the bottom of the potential energy landscape for amorphous materials. These results support the hypothesis that enhanced surface mobility allows stable glass formation by vapor deposition. A comparison of the enthalpy content of vapor-deposited glasses with aged glasses was used to evaluate the difference between bulk and surface dynamics for indomethacin; the dynamics in the top few nanometers of the glass are about 7 orders of magnitude faster than those in the bulk at $T_g - 20$ K.

Introduction

Glasses are an important class of materials. They exhibit many of the mechanical properties of crystalline solids while maintaining the disordered microscopic structure of a liquid. Glasses can be made from organic, inorganic, and metallic systems using an array of techniques[1] including physical vapor deposition[2−7] and slow cooling from the liquid. This wide breadth of materials and techniques translates into a large number of applications for glasses. For example, amorphous silicon is important for photovoltaic applications; vitreous silica is the material of choice for optical fibers; glassy polymers are heavily utilized for optical and structural applications.

One fundamental issue that remains unresolved for amorphous materials is the Kauzmann entropy crisis.[8−11] Figure 1 is a schematic that illustrates the central issue. If crystallization can be avoided as a liquid is cooled below the melting temperature T_m, the liquid becomes supercooled. As the temperature of the supercooled liquid is lowered at some rate, a temperature is reached where the system falls out of equilibrium. At this temperature, often denoted as the glass transition temperature T_g, molecular motion becomes so slow that the molecules cannot rearrange on the time scale of the experiment. Kauzmann noted that if the entropy of the supercooled liquid is extrapolated to lower temperatures, it will equal the entropy of the crystal at a temperature not too far below T_g; the temperature where this occurs is referred to as the Kauzmann temperature T_K. While it is alarming enough that an amorphous state would have the same entropy as a well-ordered crystal, further entropy decreases along the extrapolated supercooled liquid line would result in a violation of the third law of thermodynamics. Thus it is generally accepted that the entropy of a supercooled liquid cannot continue to decrease along the extrapolated path as the temperature is lowered.

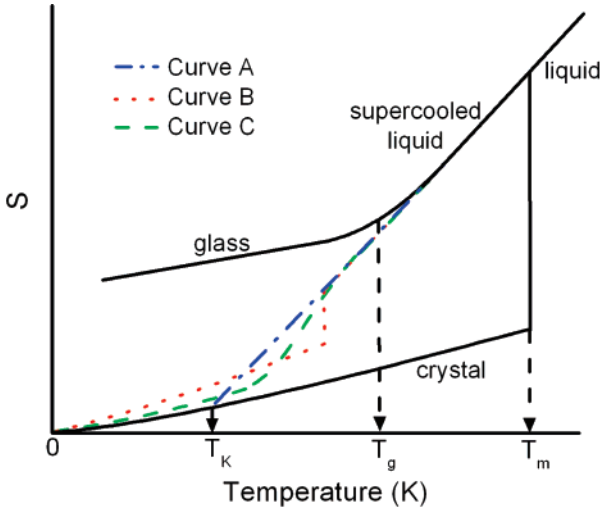

Figure 1. Schematic representation of the Kauzmann entropy crisis and some potential resolutions. The solid black lines designate regions that are currently accessible with experiments, with the vertical dashed arrows indicating the Kauzmann temperature T_K, the glass transition temperature T_g, and the melting temperature T_m. Curve A (blue, dash-dot) illustrates the entropy of the supercooled liquid extrapolated to low temperature with a transition to an ideal glass at T_K. Curve B (red, dotted) shows a possible first-order phase transition, and curve C (green, dashed) illustrates a possible resolution without a phase transition.

A number of resolutions to the entropy crisis have been proposed. Gibbs and DiMarzio[12] and subsequently Adam and Gibbs[13] proposed a second-order phase transition to an ideal glass at T_K with the ideal glass having the same entropy as the crystal; this transition is represented by curve A of Figure 1. As an alterative, a first-order phase transition has been proposed

* To whom correspondence should be addressed. E-mail: ediger@chem.wisc.edu.

† Permanent address: One Amgen Center Dr., Thousand Oaks, CA 91320.

10.1021/jp7113384 CCC: $40.75
Published on Web 04/03/2008

between T_g and T_K (curve B). Experimental evidence for such a liquid−liquid transition has been reported for triphenyl phosphite,[14,15] $Al_2O_3-Y_2O_3$,[16] and H_2O.[17] Several models have also been proposed that support a liquid−liquid transition beginning with the free volume models of Cohen and Grest,[18] along with the cooperative bond-lattice excitation models of Angell.[19−23] A further alternate resolution to the entropy crisis is a continuous curve with no phase transition (curve C shows one possible example). Curves of this type were originally obtained from two-state models[24,25] and recently have been observed in the exact numerical solutions to some model problems.[26] Results similar to curve C have also been observed in a number of simulations rooted in work on the potential energy landscape.[10,27,28] Understanding which of these resolutions (A, B, or C) is correct is important for predicting the mechanical and dynamical properties of amorphous materials above T_g. Theoretical treatments that attempt to describe dynamics above T_g often begin with an idea or assumption about the thermodynamics of supercooled liquids below the conventional T_g.[13,29−31]

In general, it has not been possible to experimentally determine how liquids resolve the entropy crisis. To do so requires access to the (metastable) equilibrium supercooled liquid at temperatures approaching T_K. While cooling a liquid more slowly maintains equilibrium to a lower temperature, molecular motions slow so precipitously as the temperature is lowered that thousands of years or more would be required to get even halfway to T_K while maintaining equilibrium.

The potential energy landscape provides a useful language to describe the entropy crisis.[10] The energy landscape controls the dynamics and thermodynamics of an amorphous N molecule system via the barrier heights and basin depths, respectively, of a surface with at least $3N + 1$ dimensions.[32−34] At temperatures far above T_g, the system has sufficient energy to cross the barriers and sample configuration space. Below T_g, the system becomes stuck on the energy landscape; molecular rearrangements do allow for new configurations, but these can only be explored very slowly. *Understanding the resolution of the entropy crisis requires access to the lower reaches of the energy landscape.* For example, if curve A of Figure 1 is correct, the supercooled liquid would reach the bottom of the amorphous portion of the energy landscape at T_K.

We have recently shown that vapor deposition can be used to quickly prepare glasses that are low on the potential energy landscape.[35,36] Highly stable glasses of 1,3,5-(tris)naphthylbenzene (TNB) and indomethacin (IMC) were formed from vapor deposition onto substrates with temperatures near 0.85 T_g. These glasses were up to 8 J/g lower in enthalpy and nearly 2% more dense than glasses prepared by cooling the liquid. The ability to create these glasses was attributed to enhanced mobility at the glass/vacuum interface where molecules can efficiently explore configuration space and thus find a lower position on the energy landscape. Until this recent work, the prevailing view in the literature was that vapor deposition results in high-enthalpy, low-density glasses.[37−41] A recent paper by Kearns et al.[36] shows that the substrate temperature is a key variable. Substrates held far below 0.85 T_g result in less stable glasses, presumably because mobility at the surface is no longer fast enough to allow configurational sampling.

Here we report how the rate of deposition changes the stability achieved during the vapor deposition process. Using both IMC and TNB, depositions were performed at substrate temperatures $T_{substrate}$ near 0.85 T_g, where enhanced surface dynamics is expected to have the largest impact on glass stability.[36] Deposition rates from 15 to 0.15 nm/s were explored. Differential scanning calorimetry (DSC) was used to characterize both the kinetic stability and the enthalpy, as quantified by the onset temperature T_{onset} for mobility and the fictive temperature T_f, respectively.

We find that both the kinetic stability and the enthalpy of vapor-deposited glasses are strongly influenced by the rate of deposition. Lowering the deposition rate by 2 orders of magnitude lowered T_f by at least 10 K in both IMC and TNB. The lowest deposition rates gave T_f values *at least 30 K below* the conventional T_g, indicating that *these glasses have moved nearly halfway to the bottom of the amorphous potential energy landscape as compared to ordinary glasses.* Additionally, the most stable IMC and TNB samples have mobility onset temperatures about 25 K higher than that of the ordinary glass produced by cooling the liquid.

The ability to make more stable IMC and TNB glasses by lowering the deposition rate supports the enhanced surface mobility mechanism and allows an estimate of surface relaxation times. Lower deposition rates allow molecules on the surface of the film more time to explore configurations and find a lower position on the potential energy landscape. By comparing the enthalpy content of glasses vapor-deposited at different rates with ordinary glasses aged for long period of times, we estimate that molecular rearrangements at the surface of an IMC glass at 295 K occur about 10^7 times more rapidly than bulk rearrangements.

Experimental Section

Materials. IMC was purchased from Sigma (St. Louis, MO) and used without further purification. The chemical purity (TLC grade) was greater than 99% and consisted of the γ crystalline polymorph. The melting temperature of the as-received material ($T_m = 432.8$ K) agreed with literature data for the γ polymorph to within 1 K.[42,43]

TNB was synthesized by McMahon and co-workers.[44] The $\alpha\alpha\beta$ isomer was used in this study. The melting temperature agreed with the published literature values for the $\alpha\alpha\beta$ isomer to within 1.5 K.[45]

Vapor Deposition. Vapor deposition was performed by heating the crystalline source material in a quartz crucible. Aluminum DSC pans were used as substrates and held 3 cm away from the source in a vacuum chamber; the base pressure of the chamber was 10^{-8} Torr. Pans were attached to a copper cold stage using Apiezon N grease to maintain good thermal contact with the stage during the deposition. The temperature of the stage was controlled to within 1 K with a Lakeshore 340 temperature controller. Platinum 4-wire RTDs (resistive temperature detector, Omega) were used to detect the temperature of the stage. Rates of deposition were monitored with a quartz crystal microbalance (QCM, Sycon Instruments) and controlled by adjusting the temperature of the crucible. For the lower deposition rates, the instantaneous deposition rate was always within 20% of the stated deposition rate. For the highest deposition rate (for IMC), the rate was ramped from 0 to 15 nm/s within the first 5 min of the deposition process and then maintained within 20%. Depositions continued until 2−4 mg of sample had been deposited into a DSC pan.

DSC Analysis. The details of the DSC analysis have been described elsewhere,[36] and only the major points will be discussed here. A TA Instruments Q1000 DSC obtained three heating scans (10 K/min) for each sample. The first scan measured the heat capacity C_p of the as-deposited glass. After this scan was complete, the sample was allowed to crystallize. The second scan determined the C_p of the crystal allowing the

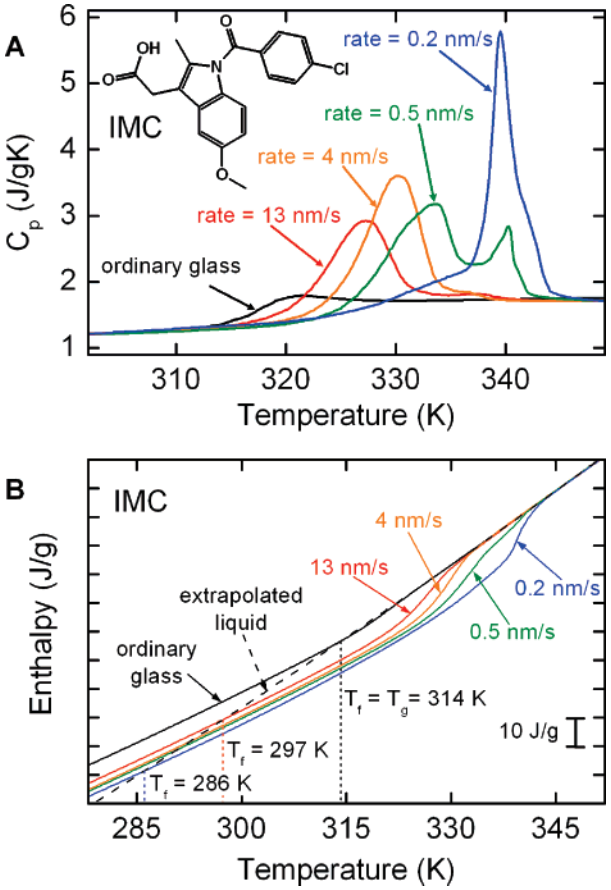

Figure 2. (A) Heat capacity curves observed for vapor-deposited IMC. $T_{substrate}$ was 265 K (0.84 T_g) for each deposition. Depositions were performed at rates of 13 nm/ s (red), 4 nm/s (orange), 0.5 nm/s (green), and 0.2 nm/s (blue). Also shown is the ordinary glass C_p curve (black), obtained after cooling the liquid at approximately 40 K/min. Inset: Structure of IMC. (B) Enthalpy curves obtained from integrating the C_p curves in part A. The color of the lines shown in part A corresponds to the curves shown in part B. The temperature at which the extrapolated liquid line (black, dashed) intersects the enthalpy of the vapor-deposited curves defines the fictive temperature T_f as indicated by the dotted vertical lines.

sample mass to be calculated from the heat of fusion. After the second scan, the sample was cooled at approximately 40 K/min into the glassy state. We refer to this glass as the "ordinary glass," and this sample is the basis of comparison with vapor-deposited glasses. The third scan measured the C_p for the ordinary glass. Throughout this paper, we refer to the onset temperature for the third scan (315 K for IMC, 348 K for TNB) as T_g, without specifying each time the particular cooling and heating rates that produce these values.

We have previously shown that the vapor-deposited material is chemically pure and that the thermomechanical and chemical properties of the substrate do not affect the observed C_p curves.[36]

Results

Influence of Deposition Rate on the Enthalpy of the Glass. Figure 2A shows the heat capacity C_p curves for IMC glasses vapor-deposited at various rates. $T_{substrate}$ is held constant at 265 K (0.84 T_g) for each of these depositions; we previously determined this to be the optimal temperature for preparing stable glasses.[36] The black curve shows C_p for the ordinary glass, with an onset temperature of 315 K. The shape of the C_p curves for the vapor-deposited samples change significantly as a function of deposition rate. The observed enthalpy overshoots

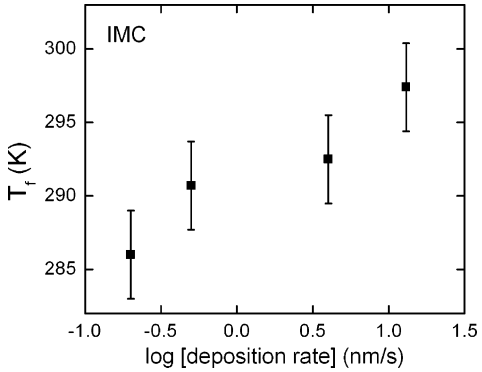

Figure 3. Summary of fictive temperatures T_f as a function of deposition rate for IMC. T_f is a single parameter measure of the enthalpy of a glass. $T_{substrate}$ was 265 K (0.84 T_g) for each deposition. Error bars indicate the standard deviations characterizing the range of T_f values obtained from three to nine samples.

(peaks in C_p) shift to higher temperatures as the deposition rate is lowered from 13 to 0.2 nm/s. The shapes of the overshoots also change with deposition rate. In particular, a double-peaked structure is observed for deposition at 0.5 nm/s; this will be discussed below.

Figure 2B shows the apparent enthalpy curves that result from integrating the C_p curves described above. After integration the curves are vertically shifted to match at a temperature in the supercooled liquid range where the thermodynamic state of all samples is the same. The enthalpies of all the vapor-deposited glasses are lower than that of the liquid-cooled ordinary glass, and the enthalpy is lowest at the lowest deposition rate.

It is convenient to compare the enthalpy of different glasses through the fictive temperature T_f. At temperatures far below T_f, the glass "structure" is fixed, and thus T_f is a one-parameter measure of the enthalpy content of the glass; lower T_f values indicate lower enthalpy content. For samples prepared by cooling the liquid, T_f approximately describes the temperature at which the liquid left equilibrium upon cooling. For vapor-deposited glasses, T_f is defined from the heating scan as the intersection between the experimentally observed enthalpy and the extrapolated supercooled liquid enthalpy (dashed line). The IMC supercooled liquid C_p is fit with Shamblin et al.'s data[46] using

$$C_p(J/gK) = 3.10 \times 10^{-3}\, T/K + 6.8 \times 10^{-1} \qquad (1)$$

The second-order polynomial that results to describe the enthalpy of the supercooled liquid is

$$H(J/g) = 1.55 \times 10^{-3}\,(T/K)^2 + 6.8 \times 10^{-1} T/K + C \qquad (2)$$

Figure 3 is a summary of the T_f values calculated for IMC vapor-deposited onto substrates held at 265 K. T_f depends strongly on deposition rate. The lowest deposition rate results in a T_f of 286 K, which is nearly *30 K below that of the ordinary glass*.

Similar data has been obtained for a second organic glass-former, TNB. Figure 4 shows both C_p data (A) and the resulting enthalpy (B). $T_{substrate}$ for these depositions was 295 K ($\approx$ 0.85 T_g) and the deposition rate was varied by a factor of 30. As for IMC, lower deposition rates produce larger enthalpy overshoots and lower enthalpy glasses. We used Magill's C_p data for supercooled TNB[47] in order to extrapolate the supercooled liquid enthalpy to lower temperatures for the purpose of calculating T_f. The equation used for C_p is

$$C_p(J/gK) = -6.31 \times 10^{-6}(T/K)^2 + 7.73 \times 10^{-3} T/K - 3.48 \times 10^{-1} \qquad (3)$$

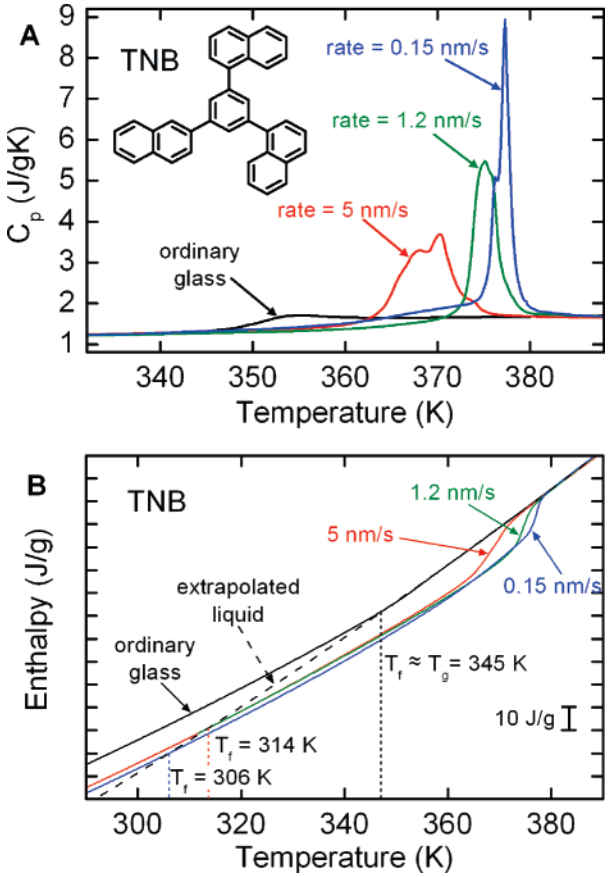

Figure 4. (A) Heat capacity curves observed for vapor-deposited TNB. $T_{substrate}$ was 295 K (0.85 T_g) for each deposition. Depositions were performed at the rates of 5 nm/s (red), 1.2 nm/s (green), and 0.15 nm/s (blue). The ordinary glass scan is obtained on a sample cooled from the liquid at approximately 40 K/min. Inset: Structure of TNB. (B) Enthalpy obtained from integrating C_p curves in part A. The color of the lines shown in part A corresponds to the curves shown in part B. The temperature at which the extrapolated liquid line (dashed) intersects the enthalpy of the vapor-deposited curves defines T_f as indicated by the dotted vertical lines.

Integrating eq 3 gives the supercooled liquid enthalpy plotted in Figure 4B, which is

$$H(\mathrm{J/g}) = -2.103 \times 10^{-6}(T/\mathrm{K})^3 + 3.865 \times 10^{-3}(T/\mathrm{K})^2 - 3.48 \times 10^{-1}(T/\mathrm{K}) + C \quad (4)$$

The T_f values for TNB calculated from Figure 4B are summarized in Figure 5. At the lowest deposition rate of 0.15 nm/s, *the calculated T_f is 40 K below T_g of the ordinary glass*. This T_f value is only 10 K higher than $T_{substrate}$.

Influence of Deposition Rate on Kinetic Stability. Figure 6 shows the kinetic stability of vapor-deposited IMC and TNB glasses as a function of deposition rate. We use the onset temperature T_{onset} to quantify the kinetic stability. Below T_{onset} the sample is too immobile to absorb the heat needed to become a liquid. At T_{onset}, the molecules begin to move, and an increase in heat capacity is observed as a consequence of configurational sampling. A higher T_{onset} signifies an increase in kinetic stability. Panel A of Figure 6 graphically defines T_{onset} as the intersection of the extrapolated glass line and the tangent drawn from the half-height of the enthalpy overshoot.

Panels B and C of Figure 6 show the deposition rate dependence of T_{onset} for IMC and TNB, respectively. For both materials, lowering the deposition rate increases T_{onset}, indicating an enhancement of kinetic stability. T_{onset} values for the slowest

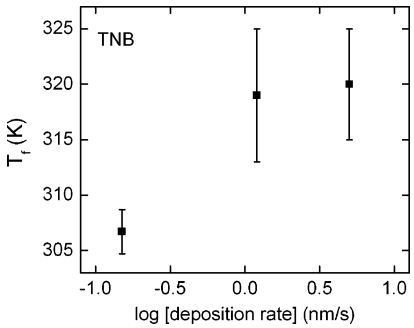

Figure 5. Summary of fictive temperatures T_f as a function of deposition rate for TNB. $T_{substrate}$ was 295 K (0.85 T_g) for each deposition. For the lowest deposition rate, the error bar indicates the range of T_f values obtained from two samples. For the two higher rates, the error bars indicate the uncertainty of the mass of sample, which was larger for these two samples.

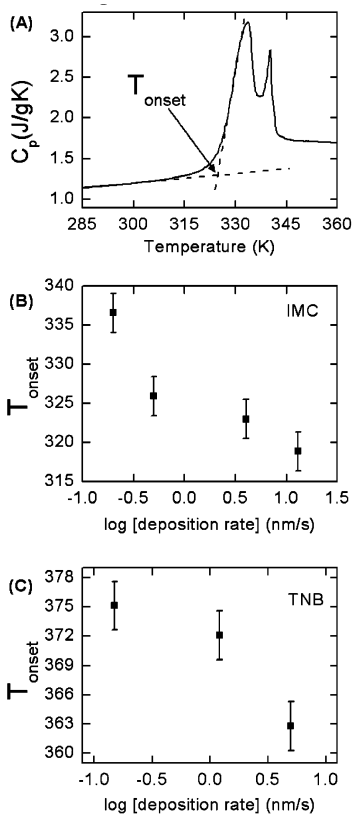

Figure 6. Kinetic stability of vapor-deposited glasses of IMC and TNB as a function of deposition rate. $T_{substrate}$ for IMC and TNB was 265 and 295 K, respectively. (A) C_p vs T is plotted for an IMC sample deposited at 265 K and a rate of 0.5 nm/s. Definition of the onset temperature T_{onset} for mobility is indicated by the intersection of the dashed lines. (B) Kinetic stability of vapor-deposited IMC glasses as indicated by T_{onset} from DSC. Error bars indicate the standard deviations characterizing the range of T_{onset} values obtained from 3−9 samples. (C) Kinetic stability of vapor-deposited TNB glasses as indicated by T_{onset}. Error bars indicate the standard deviations characterizing the range of T_{onset} values obtained from two to three samples.

deposition rates are *at least 25 K greater* than for the ordinary glass. By consideration of Figures 2−6 collectively, we note that lower depositions rates produce glasses with lower enthalpies and higher kinetic stabilities.

Two Routes to Stability: Aging vs Deposition Rate. One traditional way to produce low-energy glasses is to isothermally age a glass below T_g. Glasses are in nonequilibrium states and relax slowly toward the more thermodynamically stable super-

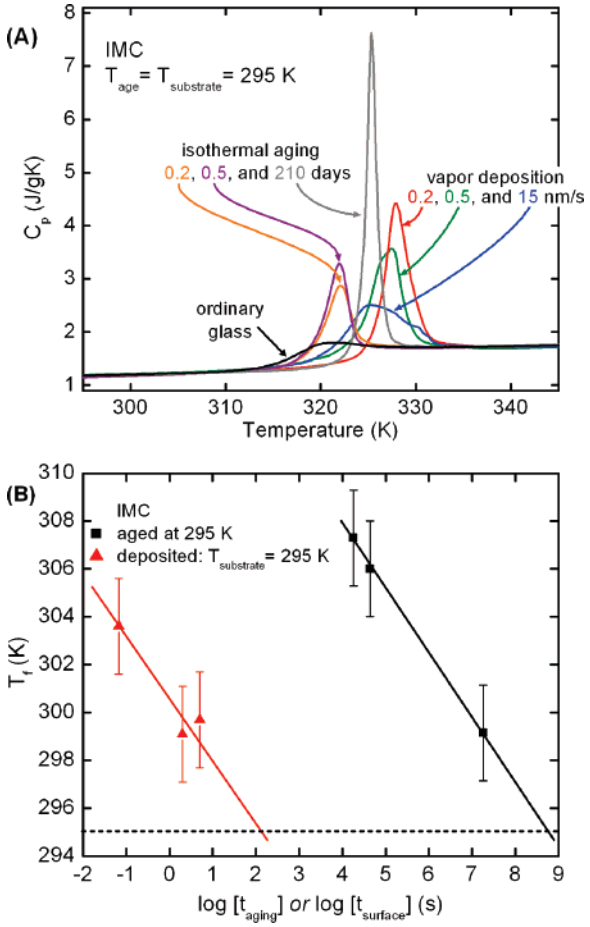

Figure 7. Comparison of aged and vapor-deposited IMC samples. (A) C_p of ordinary IMC glasses aged at 295 K for various periods of time (orange, 0.2 days; purple, 0.5 days; gray, 210 days) and C_p for vapor-deposited IMC glasses prepared with $T_{substrate} = 295$ K at various rates (blue, 15 nm/s; green, 0.5 nm/s; red, 0.2 nm/s). (B) Comparison of bulk (black squares) and surface (red triangles) equilibration times at 295 K for IMC. Solid lines are lines of best fit through the data. The dotted horizontal line indicates the T_f expected when thermodynamic equilibrium is reached. The surface equilibration time $t_{surface}$ is calculated for the vapor-deposited samples by dividing our estimate of the thickness of the mobile surface layer (1 nm) by the deposition rate.

cooled liquid. Experimentally, one can characterize the progress of a glass toward the metastable supercooled liquid state through the evolution of T_f. As glasses are aged for longer periods of time, T_f will decrease until it is equal to the aging temperature.

Figure 7A shows C_p curves for both vapor-deposited and isothermally aged IMC samples. $T_{substrate}$ for the vapor-deposited sample was 295 K, and this is also the temperature at which the ordinary IMC glass was aged. The ordinary glasses shown in the figure were aged for up to 7 months. Each aging experiment was performed with approximately 5 mg of IMC in the same type of Al pan that was used for vapor deposition. The vapor-deposited samples were deposited at rates between 15 and 0.2 nm/s. As shown in Figure 7A, the ordinary glass aged for 7 months has similar kinetic stability to a glass vapor-deposited at 0.2 nm/s. These two samples also have the same enthalpy content and thus the same T_f value (299 K). As the vapor-deposited sample described here was prepared in only 2 days, this *high kinetic stability and low enthalpy content was achieved 100 times faster in the vapor-deposited sample than in the aged ordinary glass*. Figure 7B contains a further comparison of aged and vapor-deposited glasses; it will be discussed below.

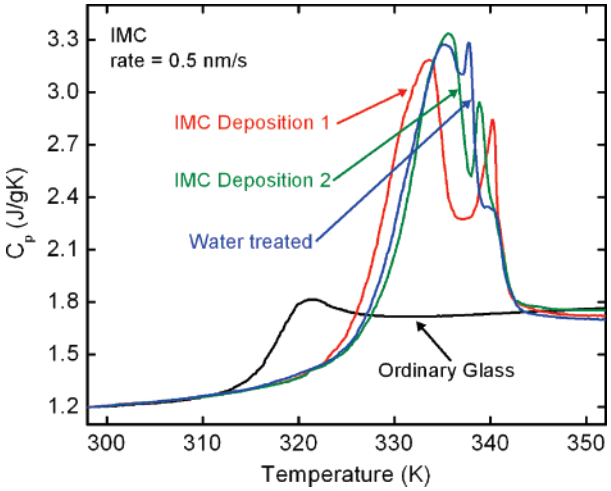

Figure 8. The effect of water treatment on the observed C_p curve for IMC. IMC was vapor-deposited with a $T_{substrate}$ of 265 K at a rate of 0.5 nm/s. Deposition 1 (red) and 2 (green) show separate depositions and indicate the reproducibility of the double-peaked structure. The water-treated sample (blue) was subjected to humid ambient air (72% RH) for 12 h and 23 h of drying at 295 K before being analyzed.

Double-Peaked C_p Curves and the Influence of Water. As shown in Figure 2, deposition rates near 0.5 nm/s produce IMC glasses that show an interesting double-peaked enthalpy overshoot. Figure 8A presents C_p curves for multiple depositions of IMC at a $T_{substrate}$ of 265 K and a deposition rate of 0.5 nm/s. For the curves labeled IMC deposition 1 and IMC deposition 2, our intent was to produce two identical samples. While there are small differences in shape and T_{onset} (perhaps due to slightly different deposition rates), both samples clearly show two peaks, indicating the reproducibility of this feature.

We also studied the effect of humidity on the observed enthalpy overshoot since amorphous IMC is slightly hygroscopic. Figure 8A shows a sample that was subjected to humid atmospheric conditions and is designated as "water treated" in the figure. Initially, this IMC sample was vapor-deposited into a DSC pan using the same conditions that produced the other two samples shown in the figure. After this sample was removed from the vacuum chamber, it was treated with ambient humid air (72% RH) for 12 h. After this exposure the sample was placed back into the vacuum chamber for 23 h at room temperature to remove any absorbed water. Finally, the redried sample was removed from the chamber, and the DSC pan was sealed and placed in dry ice to prevent additional aging at room-temperature prior to DSC analysis.

We observe that the water-treated IMC maintains a complicated enthalpy overshoot structure. A second peak is still observed, but an additional shoulder is seen at higher temperatures. It is interesting that water exposure at room temperatures for 12 h, in addition to many additional hours at room temperature, does little to the shape of the C_p curve. For comparison, Zografi and co-workers showed that water exposure drastically changed the dynamics of ordinary IMC glasses prepared by cooling the supercooled liquid.[48,49]

Water exposure also has little impact on the enthalpy content as quantified by T_f; water exposure changed the calculated T_f value by at most 2 K.

Discussion

We have shown that lowering the deposition rate increases the kinetic stability and lowers the enthalpy of vapor-deposited glasses of IMC and TNB. In this section, we rationalize our

results based on an enhanced surface mobility mechanism and describe the position of these samples on the potential energy landscape. We also discuss the origin of C_p curves with multiple peaks and whether vapor deposition might be used to prepare equilibrium liquids below the glass transition temperature.

Enhanced Surface Mobility. There are many examples in the literature where enhanced surface mobility near T_g has been observed or inferred in small-molecule[3] and polymeric systems.[50−53] Vapor deposition can utilize enhanced surface mobility to create a stable bulk glass.[35,36] Mobile molecules at the glass/vacuum interface have the opportunity to explore configuration space and reach lower positions on the potential energy landscape. As the deposition progresses, the molecules that were at the interface are buried; these molecules now relax on the much slower time scale of the bulk glass. In the meantime, new molecules arrive and rapidly sample configurations at the surface, and the process continues. Eventually this layer-by-layer process produces a bulk glass in which the molecules are locked into low-energy configurations.

The deposition rate dependence of the enthalpy and kinetic stability strongly supports this enhanced surface dynamics mechanism. Molecules that are in the mobile surface layer sample configurations until being trapped in the bulk. Lower deposition rates give the surface molecules more time for configuration sampling. Thus glasses with low enthalpies can be created as shown in Figures 2−5. These more stable local packing arrangements naturally give rise to higher onset temperatures for mobility as shown in Figure 6. Of course, this is only possible if $T_{substrate}$ is such that substantial surface mobility exists, as discussed previously.[36]

We can use the dependence of the enthalpy on the deposition rate to compare the dynamics at the surface to those in the bulk as illustrated in Figure 7B. Fictive temperatures are plotted as a function of the relevant equilibration time for vapor-deposited samples and for ordinary glasses aged for different time periods. For the aged samples, T_f is plotted against the total annealing time at 295 K (up to 210 days). For the vapor-deposited samples, we plot T_f against the surface equilibration time $t_{surface}$ since all the relevant configuration sampling occurs while the molecules are near the surface. Any bulk relaxation that may have taken place during the deposition is negligible. For this calculation, we assume that the mobile surface layer is 1 nm thick and calculate $t_{surface}$ = (1 nm)/(deposition rate). The horizontal dotted line in the graph represents the expected T_f for both samples once thermodynamic equilibrium has been reached.

Figure 7B shows that mobility at the surface of IMC glasses at 295 K is about 10^7 times faster than bulk mobility since the two solid lines are displaced by this factor. The intersection of the solid lines with the dotted line is a rough estimate of the equilibrium relaxation times for the bulk (aged data) and the surface (vapor deposition data). From this, we estimate that complete configurational sampling at the surface of an IMC glass requires about 10^2 s at 295 K. In contrast, the bulk equilibration time is estimated at roughly10^9 s.

In constructing Figure 7B, we assumed that the thickness of the mobile surface layer was 1 nm, and here we consider the impact of an error in this value. For TNB, neutron reflectivity provides a direct measurement of the thickness of the mobile surface layer.[35,54] Between $T_g - 30$ and $T_g - 50$ K, the thickness varies from 1 to 3 nm. While no similar measurements have been done on IMC, we regard this as a useful analogy, given the similarity between the two systems as shown in Figures 2−6. Other techniques also indicate mobile surface layers in the 1-nm range.[3] Since 1 nm is roughly the diameter of an IMC molecule, this is a reasonable lower bound for the thickness of the mobile surface layer. Even if we assume a 10-nm thickness for this layer, which seems unrealistically large, the left solid line in Figure 7B shifts only 1 order of magnitude to the right. Thus we regard the following as a robust conclusion: the surface of an IMC glass at 295 K is at least 10^6 times more mobile than the bulk.

Hiking down the Energy Landscape. As discussed in the introduction, glasses prepared by cooling the liquid get stuck on the potential energy landscape at T_g. Further progress down the landscape is very slow because of the extremely long time required for molecular rearrangements in a bulk glass. If we accept that an amorphous system will not have an entropy significantly lower than the crystal, then the resolution to the entropy crisis lies near the bottom of the amorphous part of the potential energy landscape, somewhere below the portion of the landscape readily accessed by traditional glasses. Vapor-deposited glasses, due to rapid configurational sampling at the glass/vacuum interface, partially circumvent this kinetic limitation.

There is a direct, quantitative relationship between the enthalpy of a glass (as determined in our experiments) and its average position on the potential energy landscape.[10] It can be shown that

$$\epsilon(\text{stable glass}) - \epsilon(\text{ordinary glass}) \approx H(\text{stable glass}) - H(\text{ordinary glass}) \quad (5)$$

where ϵ represents the average energy of the minima of occupied potential energy basins. Thus, a vapor-deposited glass whose enthalpy content is 10 J/g lower than an ordinary glass is also approximately 10 J/g lower on the potential energy landscape. Two approximations are made in deriving eq 5. First, the enthalpy is equated with the internal energy; this approximation is good to better than 0.01 J/g. Second, the internal energy is approximated as a sum of configurational and vibrational contributions, and the vibrational contributions of the two glasses are equated. Accurate comparisons of C_p for stable and ordinary glasses can determine the accuracy of this approximation; the error in eq 5 is likely to be less than 1 J/g.

We have defined a quantity θ_K that describes the position of a glass on the potential energy landscape relative to an ordinary glass that leaves equilibrium upon cooling at T_g[35]

$$\theta_K = \frac{T_g - T_f}{T_g - T_K} \quad (6)$$

When θ_K is equal to zero, a vapor-deposited sample has not progressed any further down the landscape than can be achieved by cooling the supercooled liquid at a rate on the order of 10 K /min; T_f is equal to T_g. On the other hand, a value of one indicates that a vapor-deposited glass has reached the bottom of the amorphous portion of the potential energy landscape. Equation 6 assumes that the entropy of the supercooled liquid follows curve A in Figure 1 and that the entropy of an amorphous state cannot be lower than the entropy of the crystal.

Figure 9 shows θ_K values for IMC and TNB glasses prepared by vapor deposition and by aging the ordinary glass for various periods of time. θ_K values for vapor-deposited IMC and TNB glasses deposited at the lowest rates are 0.39 and 0.42, respectively. These samples *have progressed about 40% of the way toward the bottom of the amorphous portion of the energy landscape relative to an ordinary glass.* Aging ordinary glasses of TNB or IMC below T_g for weeks to months produces glasses that are at most 24% of the way to the bottom of the landscape.

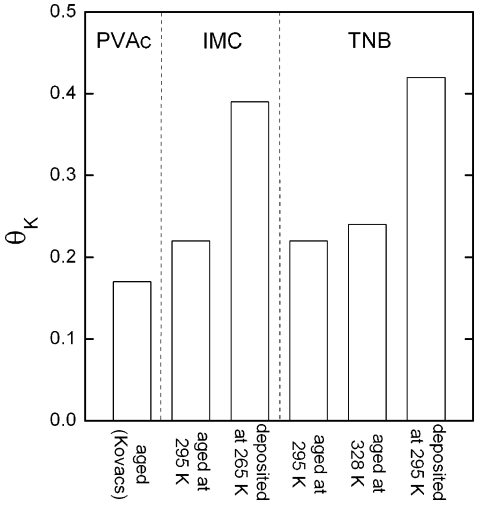

Figure 9. θ_K values for vapor-deposited and aged glasses. As explained in the text, larger θ_K values indicate glasses with lower positions on the potential energy landscape. The values indicated for the vapor-deposited IMC and TNB samples are for samples deposited at rates of 0.2 and 0.15 nm/s, respectively. The aged IMC sample was held at 295 K for 210 days. TNB was aged at 295 K for 320 days and at 328 K for 15 days. The PVAc θ_K value was determined from experiments performed by Kovacs[55] in which PVAc was annealed at 298 K for 2 months. Although vapor-deposited samples are prepared much more quickly than the aged samples, they are significantly lower on the energy landscape.

Also shown in Figure 9 is θ_K data for Kovacs' seminal aging experiments on PVAc.[55] Aging PVAc for 2 months results in a θ_K value of 0.17 or less, depending on the T_g value used.[55,56]

To provide some perspective on the θ_K values achieved by these vapor-deposited glasses, we estimate the time required to age an ordinary glass to these θ_K values. We do this calculation for TNB with $\theta_K = 0.42$ (as shown in Figure 9). Consistent with aging experiments near T_g,[57] we assume that the time required to age an ordinary glass to equilibrium is roughly equal to the equilibrium structural relaxation time (τ_α) at the aging temperature. The vapor-deposited sample has $T_f = 307$ K, and we estimate τ_α at 307 K using $\tau_\alpha = 140$ s at 344 K (based on the dielectric relaxation measurements of Richert et al.[58]) and the extrapolated temperature dependence of τ_α. Our estimate for τ_α at 307 K is 10^{19} s, 10^{12} s, or 10^{10} s, depending upon whether we use a non-Arrhenius extrapolation of the temperature dependence of the dielectric[58] and viscosity[57] data, or an Arrhenius extrapolation of the viscosity data, respectively. Thus we estimate that the time required to age an ordinary glass of TNB to the same position on the energy landscape as we have obtained by vapor deposition to be somewhere between one thousand years and one trillion years. There is no way of knowing which of these extrapolations is most realistic. In any case, as our vapor-deposited samples required less than a few days to prepare, it is clear that vapor deposition provides a route to the lower reaches of the energy landscape that is at least 10^5 times more efficient than cooling a liquid.

An unsatisfying feature of θ_K (eq 6) is that its construction assumes a particular resolution to the entropy crisis. While we can unambiguously establish the position of vapor-deposited samples on the energy landscape relative to ordinary glasses using eq 5, establishing the position relative to the bottom of the amorphous portion of the landscape necessarily involves assumptions; different resolutions to the entropy crisis will place the bottom of the amorphous portion of the landscape at different levels. An alternate method of characterizing our vapor-deposited samples uses the enthalpy of the crystal as the reference point; the crystalline state is regarded as the bottom of the energy landscape. For TNB, the ordinary glass has an enthalpy that is 58 J/g above the crystal enthalpy. The enthalpy of our most stable vapor-deposited TNB glass is 45 J/g above the crystal enthalpy. Thus this vapor-deposited sample is 22% of the way to the absolute bottom of the landscape relative to an ordinary glass.

Finally, we make a technical comment about calculations involving eq 6. For IMC and TNB, we used T_K values taken from the literature (240 K for IMC,[46] 250 K for TNB[47]). These values are within a few kelvin of the T_K values calculated from eqs 1 and 3 and the known temperature dependence of C_p for the crystals, based on the assignment of T_K as the temperature where the excess entropy is zero.[46] Some authors define T_K as the temperature where the configurational entropy goes to zero. T_K would then be 250 K for IMC and 270 K for TNB resulting in θ_K values of 0.45 and 0.53 for IMC and TNB, respectively. T_K for PVAc was taken to be equal to T_0, which is 250 K.[56]

Can Vapor Deposition Create a Low-Temperature Supercooled Liquid? To study the Kauzmann entropy crisis directly, one must create low-temperature equilibrium supercooled liquids and measure their entropy. The crisis, as usually stated, pertains to (metastable) equilibrium supercooled liquids and not nonequilibrium glass systems.[8] If equilibrium supercooled liquids can be obtained by vapor deposition, we assume that one must deposit at rates low enough that further decreasing the deposition rate does not change the properties of the sample. Under these conditions, we imagine that the molecules at the top surface of the deposited film have enough time to explore configuration space and find the equilibrium distribution of local arrangements for the temperature of the substrate. Our current range of deposition rates is limited by the 2−4 mg of sample needed for analysis with conventional DSC. Since T_f and T_{onset} are still changing with deposition rate, we assume that we have not yet reached the equilibrium supercooled liquid. We are exploring other analysis techniques that will allow us to lower the deposition rate at least another 2 orders of magnitude.

It may be that deposition into an equilibrium bulk supercooled liquid will not be possible for a given material. Figure 7A shows data for IMC samples that were either vapor-deposited with $T_{substrate}$ equal to 295 K or aged at room temperature ($\approx$295 K). These samples have similar T_f values, and yet their C_p curves have dissimilar shapes, indicating that these two glasses are not the same. This may indicate that the equilibrium local packing of molecules at the surface may differ from that in the bulk. Alternatively, the dissimilar shapes could signify that there is a much broader distribution of relaxation times for the vapor-deposited sample. Nonetheless, neither sample has yet reached thermodynamic equilibrium. Upon further aging and slower deposition, C_p curves for aged and vapor-deposited samples may overlap each other meaning vapor-deposition can produce equilibrium bulk supercooled liquids.

We have made efforts to vapor-deposit IMC glasses at even lower deposition rates. Preliminary results indicate that the trend for T_{onset} shown in Figure 6B continues, while the trend for T_f shown in Figure 3 does not. A single deposition of IMC at a rate of 0.08 nm/s with a $T_{substrate}$ of 265 K was attempted. The T_f calculated for this sample was approximately 10 degrees higher than that deposited at 0.2 nm/s, while a sharpening of the enthalpy relaxation peak was also observed. Clearly this behavior needs to be carefully explored for a number of different materials in order to understand under what circumstances vapor deposition can prepare equilibrium supercooled liquids. Unfortunately, the mass limitations of conventional DSC make it

unsuitable for these low deposition rates. As mentioned above, new techniques are being explored to circumvent this limitation.

Origin of C_p Curves with Multiple Peaks. Figures 2 and 4 show that vapor deposition of both IMC and TNB can result in glasses that have C_p curves with complex shapes. In particular, IMC with $T_{substrate}$ at 265 K and a rate of 0.5 nm/s results in a double-peaked structure as shown in Figures 2 and 8. We believe that these two peaks are an indication of two different types of local packing in the vapor-deposited glass. In this scenario, the peak at higher temperature corresponds to a more stable structure that does not "melt" into the liquid until a higher temperature. We are currently exploring other techniques to determine if indeed two different local packings are present in the sample.

In terms of the potential energy landscape, C_p curves with peaks could perhaps indicate that we are approaching the bottom of the landscape. At low positions in the landscape, the system can only sample low-energy configurations. For low enough energies there may be only a few possible local packings. If only two types of local packing were possible, this would explain an enthalpy overshoot with two distinct peaks.

Conclusions

Physical vapor deposition was used to prepare glasses of two organic molecules: IMC and TNB. The substrate temperature was held at 0.85 T_g for most experiments, and the deposition rates varied from 13 to 0.15 nm/s. The enthalpy and kinetic stability for each glass was quantified by determining the fictive temperature T_f and the mobility onset temperature T_{onset}. The slowest deposition rates resulted in the lowest enthalpies and the greatest kinetic stabilities. Vapor deposition can create low-energy glasses much more rapidly than aging. For TNB depositions at 0.85 T_g, we have progressed more than 40% of the way to the bottom of the amorphous portion of the potential energy landscape with samples that required only a few days to prepare. We estimate that aging an ordinary glass to a similar position on the landscape would require between one thousand and one trillion years, depending upon assumptions about structural relaxation in low-temperature supercooled liquids.

We attribute the ability to create these stable vapor-deposited samples to a surface layer with enhanced mobility. We estimate that the dynamics at the glass/vacuum interface of IMC are about 7 orders of magnitude faster than bulk dynamics at 295 K. The surface mobility mechanism is consistent with the T_f and T_{onset} trends observed as a function of deposition rate. Lower deposition rates allow more sampling of configurations at the surface and allow lower positions to be explored on the potential energy landscape. The ability of vapor deposition to prepare glasses low on the energy landscape opens up the possibility of experimentally determining how the Kauzmann entropy crisis is avoided.

Exposing a stable IMC glass to a humid environment for 12 h resulted in little change to the C_p curves, the enthalpy content, and the kinetic stability of the glass. For both organic light-emitting diode (OLED) and pharmaceutical applications, producing amorphous materials that are stable against environmental perturbations is important. Changes to the absorption spectrum of amorphous Alq_3 films, a system often used in OLEDs, have been observed after exposure to ambient atmospheric conditions.[59,60] Andronis et al.[48,49] showed that crystallization rates in amorphous IMC greatly increased when water vapor was present in the sample. We are currently studying water uptake in IMC glasses to determine the extent to which vapor-deposited glasses might better resist environmental changes.

Acknowledgment. This work was supported by the National Science Foundation (CHE-0605136).

References and Notes

(1) Angell, C. A. *Science* **1995**, *267*, 1924.
(2) Greer, A. L. *Science* **1995**, *267*, 1947.
(3) Bell, R. C.; Wang, H. F.; Iedema, M. J.; Cowin, J. P. *J. Am. Chem. Soc.* **2003**, *125*, 5176.
(4) Stevenson, K. P.; Kimmel, G. A.; Dohnalek, Z.; Smith, R. S.; Kay, B. D. *Science* **1999**, *283*, 1505.
(5) Ayotte, P.; Smith, R. S.; Teeter, G.; Dohnalek, Z.; Kimmel, G. A.; Kay, B. D. *Phys. Rev. Lett.* **2002**, *88*, 245505.
(6) Mapes, M. K.; Swallen, S. F.; Kearns, K. L.; Ediger, M. D. *J. Chem. Phys.* **2006**, *124*, 054710.
(7) Shirota, Y. *J. Mater. Chem.* **2000**, *10*, 1.
(8) Kauzmann, W. *Chem. Rev.* **1948**, *43*, 219.
(9) Speedy, R. J. *Biophys. Chem.* **2003**, *105*, 411.
(10) Stillinger, F. H. *J. Chem. Phys.* **1988**, *88*, 7818.
(11) Stillinger, F. H.; Debenedetti, P. G.; Truskett, T. M. *J. Phys. Chem. B* **2001**, *105*, 11809.
(12) Gibbs, J. H.; DiMarzio, E. A. *J. Chem. Phys.* **1958**, *28*, 373.
(13) Adam, G.; Gibbs, J. H. *J. Chem. Phys.* **1965**, *43*, 139.
(14) Kurita, R.; Tanaka, H. *Science* **2004**, *306*, 845.
(15) Tanaka, H.; Kurita, R.; Mataki, H. *Phys. Rev. Lett.* **2004**, *92*, 025701.
(16) Aasland, S.; McMillan, P. F. *Nature* **1994**, *369*, 633.
(17) Poole, P. H.; Sciortino, F.; Essmann, U.; Stanley, H. E. *Nature* **1992**, *360*, 324.
(18) Cohen, M. H.; Grest, G. S. *Phys. Rev. B* **1979**, *20*, 1077.
(19) Angell, C. A.; Rao, K. J. *J. Chem. Phys.* **1972**, *57*, 470.
(20) Angell, C. A.; Moynihan, C. T.; Hemmati, M. *J. Non-Cryst. Solids* **2000**, *274*, 319.
(21) Moynihan, C. T.; Angell, C. A. *J. Non-Cryst. Solids* **2000**, *274*, 131.
(22) Matyushov, D. V.; Angell, C. A. *J. Chem. Phys.* **2005**, *123*, 034506.
(23) Matyushov, D. V.; Angell, C. A. *J. Chem. Phys.* **2007**, *126*, 094501.
(24) Angell, C. A.; Wong, J. *J. Chem. Phys.* **1970**, *53*, 2053.
(25) Macedo, P. B.; Capps, W.; Litovitz, T. A. *J. Chem. Phys.* **1966**, *44*, 3357.
(26) Brangian, C.; Kob, W.; Binder, K. *J. Phys. A* **2003**, *36*, 10847. Wolfgardt, M.; Baschnagel, J.; Paul, W.; Binder, K. *Phys. Rev. E* **1996**, *54*, 1535.
(27) Saika-Voivod, I.; Poole, P. H.; Sciortino, F. *Nature* **2001**, *412*, 514. Saika-Voivod, I.; Sciortino, F.; Poole, P. H. *Phys. Rev. E* **2004**, *69*.
(28) Saksaengwijit, A.; Reinisch, J.; Heuer, A. *Phys. Rev. Lett.* **2004**, *93*, 235701.
(29) Diezemann, G.; Mohanty, U.; Oppenheim, I. *Phys. Rev. E* **1999**, *59*, 2067.
(30) Viot, P.; Tarjus, G.; Kivelson, D. *J. Chem. Phys.* **2000**, *112*, 10368.
(31) Xia, X. Y.; Wolynes, P. G. *Phys. Rev. Lett* **2001**, *86*, 5526.
(32) Debenedetti, P. G.; Stillinger, F. H. *Nature* **2001**, *410*, 259.
(33) Stillinger, F. H. *Science* **1995**, *267*, 1935.
(34) Stillinger, F. H.; Weber, T. A. *Science* **1984**, *225*, 983.
(35) Swallen, S. F.; Kearns, K. L.; Mapes, M. K.; Kim, Y. S.; McMahon, R. J.; Ediger, M. D.; Wu, T.; Yu, L.; Satija, S. *Science* **2007**, *315*, 353.
(36) Kearns, K. L.; Swallen, S. F.; Ediger, M. D.; Wu, T.; Yu, L. *J. Chem. Phys.* **2007**, *127*, 154702.
(37) Hikawa, H.; Oguni, M.; Suga, H. *J. Non-Cryst. Solids* **1988**, *101*, 90.
(38) Ishii, K.; Nakayama, H.; Okamura, T.; Yamamoto, M.; Hosokawa, T. *J. Phys. Chem. B* **2003**, *107*, 876.
(39) Oguni, M.; Hikawa, H.; Suga, H. *Thermochim. Acta* **1990**, *158*, 143.
(40) Takeda, K.; Yamamuro, O.; Oguni, M.; Suga, H. *Thermochim. Acta* **1995**, *253*, 201.
(41) Takeda, K.; Yamamuro, O.; Suga, H. *J. Phys. Chem.* **1995**, *99*, 1602.
(42) Crowley, K. J.; Zografi, G. *J. Pharm. Sci.* **2002**, *91*, 492.
(43) Wu, T.; Yu, L. *J. Phys. Chem. B* **2006**, *110*, 15694.
(44) Bonvallet, P. A.; Breitkreuz, C. J.; Kim, Y. S.; Todd, E. M.; Traynor, K.; Fry, C. G.; Ediger, M. D.; McMahon, R. J. *J. Org. Chem.* **2007**, *72*, 10051.
(45) Whitaker, C. M.; McMahon, R. J. *J. Phys. Chem.* **1996**, *100*, 1081.
(46) Shamblin, S. L.; Tang, X. L.; Chang, L. Q.; Hancock, B. C.; Pikal, M. J. *J. Phys. Chem. B* **1999**, *103*, 4113.
(47) Magill, J. H. *J. Chem. Phys.* **1967**, *47*, 2802.
(48) Andronis, V.; Yoshioka, M.; Zografi, G. *J. Pharm. Sci.* **1997**, *86*, 346.
(49) Andronis, V.; Zografi, G. *Pharmaceut. Res.* **1998**, *15*, 835.
(50) Ellison, C. J.; Torkelson, J. M. *Nature Mater.* **2003**, *2*, 695.
(51) Forrest, J. A.; Dalnoki-Veress, K.; Stevens, J. R.; Dutcher, J. R. *Phys. Rev. Lett.* **1996**, *77*, 2002.

(52) Kawana, S.; Jones, R. A. L. *Phys. Rev. E* **2001**, *6302*, 021501.
(53) Keddie, J. L.; Jones, R. A. L.; Cory, R. A. *Faraday Discuss.* **1994**, *98*, 219.
(54) Swallen, S. F.; Mapes, M. K.; Kim, Y. S.; McMahon, R. J.; Ediger, M. D.; Satija, S. *J. Chem. Phys.* **2006**, *124*, 184501.
(55) Kovacs, A. J. *Fortschr Hochpolym.-Forsch.* **1963**, *3*, 394.
(56) Richert, R. *Physica A* **2000**, *287*, 26.
(57) Plazek, D. J.; Magill, J. H. *J. Chem. Phys.* **1966**, *45*, 3038.
(58) Richert, R.; Duvvuri, K.; Duong, L.-T. *J. Chem. Phys.* **2003**, *118*, 1828.
(59) Kwong, C. Y.; Djurisic, A. B.; Roy, V. L.; Lai, P.; Chan, W. K. *Thin Solid Films* **2004**, *458*, 281.
(60) Djurisic, A. B.; Kwong, C. Y.; Guo, W. L.; Lau, T. W.; Li, E. H.; Liu, Z. T.; Kwok, H. S.; Lam, L. S. M.; Chan, W. K. *Thin Solid Films* **2002**, *416*, 233.